RXTE observations of GS 1354–644 recurrent X-ray Nova outburst

Mikhail G. Revnivtsev[1,2], Konstantin N. Borozdin[2,1], William C. Priedhorsky[2], Alexey Vikhlinin[3]

[1] – Space Research Institute, Moscow, Russia

[2] – Los Alamos National Laboratory, Los Alamos, NM 87545, USA

[3] – Harvard-Smithsonian Center for Astrophysics, Cambridge, MA 02138, USA

ABSTRACT

We present the results of Rossi X-ray Timing Explorer observations of GS 1354–644 during its 1997–1998 modest outburst. The source is one of a few black hole X-ray transients, which is confirmed to be recurrent, i.e. more than one X-ray outburst was detected. Previous outburst of the same source observed with Ginga in 1987 was much brighter, and the source was found in high/soft spectral state. In 1997-1998 GS1354-644 was clearly in another typical for black hole binaries spectral state - hard/low. Total duration of the outburst was 150-200 days in RXTE/ASM band. PCA and HEXTE observations cover ∼70 days close to the maximum of the light curve and during the flux decline. The overall power-law like spectrum shape did not change during the observations and can be approximated by models of up-scattering of soft photons by energetic electrons in a hot plasma cloud with the temperature kT ∼30 keV and optical depth τ ∼4–5 (for spherical geometry). For good fit of the data an addition of an iron fluorescent line and a reflection component is required, which indicates the presence of optically thick cool material, most probably in outer part of the accretion disk. Dramatic fast variability was observed, and has been analyzed in the context of a shot noise model. The shape of power spectrum was typical for black hole systems in low/hard state. We note a qualitative difference in the shape of the fractional variability versus energy dependence, comparing systems with black holes and with neutron stars. Since it is difficult to discriminate these systems on spectral grounds, at least in their low/hard states, this new difference might be important for discriminating black holes and neutron stars.

1. Introduction

A modest X-ray outburst from the recurrent transient X1354–644 was detected by the All Sky Monitor (ASM) aboard the Rossi X-ray Timing Explorer (RXTE) around Nov.1,

1997 (Remillard, Marshall & Takeshima 1998). The flux from the source measured by ASM in 2-12 keV energy rose gradually up to 40-50 mCrab in mid-November, stayed at this level for about a month and then started to decline slowly. The maximal hard X-ray flux observed by BATSE (Harmon & Robinson 1998) and HEXTE (Heindl et al. 1997) appeared to be around 150 mCrab, indicating a hard spectrum, with an exponential cutoff detected by HEXTE at higher energies.

Following the detection of the source in X-rays, B- and R-band images were obtained (Castro-Tirado et al. 1997). The optical counterpart BW Cir has been found in a bright state. Radio (Fender et al. 1997) and infrared (Soria, Bessell & Wood 1998) emission was also detected during the X-ray outburst. Spectroscopic observations of this transient, obtained in Jan, 1998, reveal the emission of a strong H-alpha line, with the profile which varied from double- to single-peaked over the three nights of observation, reminiscent of the behavior of the black hole candidate GRO 1655-40 during its 1996 outburst, and strongly suggestive of an origin in an accretion disk (Buxton et al. 1998).

The X-ray transient source X1354–644 belongs to the class of X-ray binaries known as X-ray Novae (e.g. Sunyaev et al. 1994; Tanaka & Shibazaki 1996). All sources of this class are assumed to be recurrent, but for few of them has more than one outburst been observed by X-ray experiments. In case of X1354–644, thanks to the discovery of an optical counterpart in 1987 (Pedersen, Ilovaisky & van der Klis 1987) and its observations in 1997 (Castro-Tirado et al. 1997), one can reliably identify the source detected in 1997 with one observed by Ginga in 1987 as GS1354–64(Makino 1987, Kitamoto et al. 1990). It is quite probable, that the X-ray emission from the same source, under different names, was detected also in 1967 (Harries et al. 1967, Francey 1971), in 1971-1972 (Markert et al. 1977), and in 1974-1976 (Seward et al. 1976; Wood et al. 1984). Those earlier observations however are more disputable, because of relatively poor (order of degree) localization accuracy for the source of X-ray signal and the lack of an information about counterparts in other wavelengths.

Different outbursts of the source varied by orders of magnitude in peak flux. The most prominent outburst was one detected in 1967 as Cen X-2 (Harries et al. 1967). It is worth noting that Cen X-2 was the first X-ray transient found and one of the brightest Galactic X-ray sources known. The peak fluxes detected by Ginga in 1987 (Kitamoto et al. 1990) and by OSO-7 in 1971-1972 (Markert et al. 1977) were about 2 orders of magnitude weaker in comparison with maximum of Cen X-2 outburst. Maximal flux detected by RXTE in 1997 was about 3 times lower than maximum of 1987 outburst.

The energy spectra detected during different outbursts of the system were also quite different. The spectrum measured with Ginga in 1987 was composed of a strong soft

component below 10 keV and a power law at higher energies, which is typical for black-hole binaries in their "high" spectral state. In contrast, the spectrum detected by RXTE in the current outburst is typical for "low" spectral states of Galactic X-ray binaries.

In this paper we present an analysis of the observations of GS1354–644 during its 1997-1998 outburst by RXTE experiments. Overview of observations and data reduction approach is presented in section 2. Timing analysis is presented in §3, spectral analysis in §4. Comparisons with data from other sources and against some theoretical models are presented mainly in section 5. Main results are summarized in §6.

2. Observations and data reduction

Rossi X-ray Timing Explorer satellite (Bradt, Rothschild & Swank 1993) has two coaligned spectrometers, PCA and HEXTE, with narrow fields of view, and an All Sky Monitor (ASM). PCA and HEXTE together provide broad band spectral coverage for an energy range from 3 to $\sim$ 200 keV. ASM can trace the long term behavior of the source in a 2-12 keV energy band. The data for our analysis have been obtained from the RXTE Guest Observer Facility at GSFC, which is a part of High Energy Astrophysics Science Archive Research Center (HEASARC). ASM light curves have been used as provided by RXTE GOF.

The reduction of PCA and HEXTE data was performed with standard *ftools* package. To estimate the PCA background we applied $L7/240$ background model, which takes into account various particle monitors and the SAA history, for the observation of the source at Nov 17, 1998. The background for other observations was estimated with use of VLE (Very Large Events) based model.

We have used PCA response matrix v.3.3 (Jahoda 1998 a, b). The analysis of the Crab nebula spectra confirmed, that the systematic uncertainties of the matrix were less than 1% in 3-20 keV energy band. The uncertainties in the response and a sharp decrease of PCA effective area below 3 keV makes it hard to measure low-energy absorption in the spectra accurately enough. We have used PCA data in 3-20 keV range only, and added 1% of systematic error for each PCA channel to account for the residual uncertainty in the knowledge of spectral response. All spectra had been corrected for dead-time according to Zhang & Jahoda (1996).

The response matrix v.2.6 was used when fitting the HEXTE spectra (Rothschild et al. 1998). The background value for each cluster of HEXTE detectors was estimated using the data of off-source observations. An upper energy limit for the data was defined according

to the brightness of the source. Typically, we did not consider data for energies higher than $\sim 150 - 200$ keV, where background subtraction uncertainties became unacceptably large in comparison with the source intensity. Dead-Time correction was applied to all observations.

Brief information about the pointed RXTE observations of the source is presented on Table 1. The observations of PCA and HEXTE were carried out near the peak of the source activity in X-rays, and covers both rise phase and decline phases of the outburst of 1997. During the observation of Nov 1998 the source was much dimmer, probably in the quiescent state or in the transition to the quiescence.

3. Variability

3.1. Light curve of the outburst

The light curve of the 1997 outburst was of triangular shape, possibly with a short plateau near the maximum similar to that observed from other X-ray transients (e.g. Lochner & Roussel-Dupre 1994; Harmon et al. 1994). For general light curve morphologies see Chen, Shrader & Livio 1997. The light curve of the source in the 2-12 keV energy band measured by ASM is presented in Fig.1. If approximated by an exponential function, the rise time parameter is 20 ± 2 days and decay time parameter around 40 days. Flux measurements by PCA in 2-30 keV energy band and by HEXTE in 20-100 keV energy band are shown at the same Figure. Some evidence for a secondary maximum or "kick" typical for outbursts of X-ray Novae (e.g. Sunyaev et al. 1994; review in Tanaka & Shibazaki 1996) can be noted. The light curve of the previous outburst of this source, traced by Ginga ASM, had a plateau and a decline with time scale around 60 days (Kitamoto et al. 1990). Peak flux of 1997-1998 outburst as approximated for 1-10 keV band from PCA data was equal to $\sim 1.1 \times 10^{-9}$ erg s^{-1} sm^{-2}, which is almost three times lower than the maximal flux detected with Ginga in 1987 (Kitamoto et al. 1990).

3.2. Fast variability

Strong variability of the flux was detected in the PCA observations as illustrated by the Fig.2. The flux from the source was changeable with a factor of 2-3 in 10–20 s. Since work by Terrell 1972 such a variability is often considered under the framework of shot noise model, where the light curve is made up of randomly occurring discrete and identical events, the shots. The approach was further developed by Sutherland, Weisskopf & Kahn 1978, and has been proven to be quite useful for the interpretation of data for generic

black hole candidate Cyg X-1 (Lochner, Swank & Szymkowiak 1991) and other sources, in particular black hole binaries in their low state. We shall discuss below the implementation of this model to GS1354–644 data.

Another approach to study fast variability is by means of Fourier techniques (see detailed discussion in van der Klis 1989), in particular, analysis of the power density spectra (PDS). PDSs measured with PCA during observations of GS1354–644 can be qualitatively described as a composition of at least two band-limited components, each of them looks like constant below the break frequency for this component, and power-law with a slope ∼-2 above this break frequency. PDSs for observations #3 and #9 are shown in Fig.3. The power spectra have been normalized to squared fractional rms according to Belloni & Hasinger (1990). A logarithmic rebinning in frequency has been applied to the power spectra. The white-noise level due to Poissonian statistics as modified by dead-time effects was subtracted. We have plotted PDSs as $f \times \left(\frac{rms}{mean}\right)^2$ vs. frequency. As was argued, e.g. by Belloni et al. (1997), this convention has important advantages, namely, a plot gives a direct visual idea of the rms distribution, and Lorentzian functions representing band-limited noise become symmetric in log-log plot. This convention was used for the plot only, while all analytic fits (see below) were performed on the original power spectra.

We fitted PDS by a sum of functions $\sim \frac{1}{1+(\frac{f}{f_{br}})^2}$, which represents power spectrum expected from single type of exponential shots with a profile $s(t) \sim exp(\frac{-(t-t_0)}{\tau})$, for $t > t_0$, $\tau = 1/(2\pi f_{br})$. PDSs for observations 5–9 are fitted satisfactorily by two such components, but for the first four observations the third, intermediate, component should be included to obtain a good quality of the data approximation. The fitting parameters for all components are presented on Table 2. The model and inferred parameters is very close to what was detected for other black holes (e.g. Nowak et al. 1999a; Nowak, Wilms & Dove 1999; Grove et al. 1998) and neutron stars (e.g. Olive et al. 1998a) in low state. The position of the first break in PDS evolved significantly with time - it was at lowest frequencies near the maximum of the flux and shifted to higher frequencies later. The position of last break, however, remained pretty stable.

The energy resolved power density analysis showed, that f_{break} frequencies on the PDSs in different energy bands are consistent with each other (in the range of $\sim 1-2\sigma$), similar to what observed for Cyg X-1 (e.g. Nowak, Wilms & Dove 1999) and other black hole candidates.

The dependence of integrated fractional variability versus energy in the full analyzed frequency range (10^{-3}–50 Hz) is presented in Fig.4a. The decline of integrated rms with energy detected for GS1354–644 will be discussed in more detail in next section and, in

comparison with data from other sources, in section 5.3.

3.3. Shot noise model

The strong chaotic variability had been detected in many Galactic binaries when observed in their hard/low spectral state. Following the approach developed by Terrell 1972 for Cyg X-1 data, such a variability can be modeled in terms of a shot noise model (e.g. Lochner, Swank & Szymkowiak 1991 and references therein). In the shot noise model the light curve of the source is assumed to be composed of a number of individual shots or micro flares. In principle, different shots may influence each other and may have various shapes and spectra. Some assumptions are usually accepted to simplify the model and to reduce the number of parameters. We can assume that there is only a restricted number of different types of shots, and that all shots of the same type are identical. The calculation of statistical values for the observed light curve allows the determination of some shot parameters in this simplified model. For GS1354–644 the overall shape of the power density spectrum suggests that the light curve is formed by two or three different types of shots with characteristic times corresponding to the breaks in PDS $\tau = 1/(2\pi f_{br})$(see Table 2).

Power density spectrum does not provide us with complete information about shots, because it is not possible to determine shot rates and their intensities independently. To obtain additional information we analyzed flux density distribution. The probability distribution for the flux values integrated over a 16-sec intervals is presented in Fig.5. We selected 16 sec time intervals to study long shots distribution. PDS shows that long shots and short shots give almost equal input into integrated fractional variability of the source, but the contribution of short shots into source variability is negligible below frequencies of about 0.1 Hz. Number of short shots in each 16-sec interval is large enough, so that their sum contribution to each bin is expected to be very close to constant. To avoid the influence of Poissonian counting statistics on the actual shape of the distribution, we have chosen the flux bins to be 2 times wider than the value of the Poissonian error associated with each bin.

For high shot rates one would expect that the distribution, according to the central limit theorem, would be of symmetrical Gaussian shape. However, this is not the case for our distribution, which has a detectable deficit at lower fluxes. This shape suggests low shot rate, and can be fitted by a Poissonian distribution if the duration of any single shot is substantially shorter than the time of flux integration. For GS1354–644 the first PDS component corresponds to time scales of 2-5 seconds, while the flux has been integrated over 16-sec intervals. We have assumed that the total flux from the source is a sum of constant

component, which is stable on time scale of one observation, and a variable component formed by individual shots. As was mentioned above short shots give the contribution to the constant component, so the flux variations detected are caused by long shots only. We have fitted the flux density distribution as generated by the sum of constant and variable components applying a maximum likelihood method, which is preferable compared with chi-square statistics for the measurements of low event rates. The obtained best fit parameter for the shot rate was $\simeq 0.3$ shots per second, and the best fit of the fraction of flux contributed by the constant component was in the range of 50–70%. The signal detected from an individual shot by PCA detectors was estimated to be ∼500 cnts/shot for the first observation and ∼200 cnts/shot for the last one related to the outburst of 1997. The best fit obtained for the observation 4 is presented in the Fig.5. We repeated the analysis for 64 seconds integration time and obtained consistent results. The low shot rate for long shots shows that the variability of the source on time scales of tens of seconds is caused by relatively rare powerful flares with large energy release.

Unfortunately, we were not able to study the contribution of short shots by the same method, because the flux distribution for time scales of tenths of a second depends strongly on both short and long shots contribution. However, the value of the integrated rms of the short shots with some simple constraints on the shot amplitude allows us to estimate the shots overlapping parameter using the method described in Vikhlinin et al. 1995 and consequently derive the shot rate. Thus, short shots rate can be estimated to be at the level of ∼10-15 shots/s.

The physical origin for the shots is not very clear. For GS1354–644, as well as for other black hole systems in low state, break frequencies detected in PDS (∼1 Hz) are much lower than would naturally to be expected for the environment close to a stellar mass black hole ($\sim 10^3$ Hz). The shape of the energy spectrum, which is dominated by the Comptonized emission component, moves us to explore whether the Comptonization might be a process responsible for the time blurring of intrinsicly short shots. The detected dependence of fractional variability on energy (Fig.4a) at first glance seems to support this interpretation, because photons of higher energy undergo in average more interactions and so must have a wider distribution in time and lower integral variability. However, the fractional variability integrated up to the lowest break in PDS should not be affected by this mechanism and should therefore be independent of energy. We checked this assumption for GS1354–644, but found that slope of the dependence of rms vs energy for the frequencies below 0.02 Hz (see Fig.4b) cannot be defined accurately enough. To get more definitive answer we had to repeat our analysis for observation of much brighter source, Cyg X–1, which in many ways is a prototype for GS1354–644. For this object we can clearly see, that the fractional variability of the source is decreasing with energy both when integrated up to 50

Hz, and when integrated for the frequency range below 0.2 Hz. This last result is in direct contradiction with an assumption that the Compton up-scattering might be responsible for the typical break frequencies in PDS of black hole sources in hard state, and supports the conclusion that the typical times of several tens of seconds are too long to be explained by such a mechanism.

3.4. Time lags in GS1354-644

Another way to study rapid fluctuations in the flux is to compute time lags between variations in different energy bands. We calculated frequency dependent phase lags according to the procedure applied, e.g., by Nowak et al. (1999a). Due to the weakness of the source we were forced to sum almost all of the data available – from observation #2 to #9 – to obtain the significant result. The total integrated live time of PCA observations was $\sim$ 48 ksec. In order to increase the sensitivity for the phase lag detection we analyzed the lag distribution function. Error values were estimated according to the width of the distribution. The result is presented in the Fig. 6. One can see that qualitatively the phase lag vs. Fourier frequency dependence is very similar to what was observed in low states from other X-ray binaries, both with black holes and neutron stars components (see e.g. Nowak et al. 1999a, Grove et al. 1999, Ford et al. 1999).

4. Energy spectrum

Energy spectrum of GS 1354–644 during its 1997 outburst can be roughly represented as hard power law with a slope α $\sim$1.5, with high-energy cutoff above $\sim$50 keV. Such spectra are typical for black hole binaries in a hard/low spectral state. Commonly accepted mechanism for the generation of the hard radiation in this state is thermal Comptonization (Shapiro, Lightman & Eardley 1976; Sunyaev & Titarchuk 1980). Applying the thermal Comptonization model to the hard-state BH spectra suggests the presence of a hot cloud surrounding the central object (BH) with typical plasma temperature $\sim$50 keV and Thomson optical depth $\gtrsim$1. Such a cloud is able to Comptonize soft photons which originate in the central region, most possibly - from the accretion disk.

We have fitted the spectrum by a variety of models, from the simple power law up to Comptonization models, which suggest some underlying physics under them. The results are presented on Table 3. Fits based on HEXTE data only are presented on Table 4. We present results for groups of observations (2-5 and 6-9), because spectral parameters within

each group were not significantly different for single observations, but summing them up allows us to get more accurate estimations of the parameters. The spectra for observations 2-5 and also for observation #10 are presented in Fig.7. Y-axis is in units of photon flux, multiplied by energy square. The plot in these units shows directly the energy deposition in the spectra. Crab spectrum shown in these coordinates would be close to constant, and typical spectra of Galactic black hole binaries had negative slope when in high state, and positive (up to ∼100 keV) in low state.

In the combined approximation of PCA and HEXTE data we found that cross-calibration uncertainties of these instruments plays some role. Namely, any power laws (with high energy cutoff) approximations gave noticeably different photon index values, even if the same energy bands were used. Thus, following the approach by Wilms et al. 1999 for PCA and HEXTE spectra we used power laws with photon indexes differed by 0.08-0.1. In the Table 3 we present the PCA photons indexes.

Results of the fitting show clearly that the spectrum demonstrate noticeable high energy cut-off of power-law at the energies above ∼60 keV. In spite of that different models give the different cut-off parameters, no fit without such cut-off was found to be satisfactory. Also, the spectrum cannot be fully described by a simple power law, with or without a high energy cut-off. The spectral fit is improved significantly by the addition of a neutral iron fluorescent line and a reflection component which is an indication that part of the emission is reflected by optically thick cold material, most probably in outer part of the accretion disk (Basko, Sunyaev & Titarchuk 1974; George & Fabian 1991; Magdziarz & Zdziarski 1995). During the fitting this component was represented by *pexrav* model of $XSPEC$ package (reflection from the neutral medium).

Among Comptonization models we have applied the classical *compST* model by Sunyaev & Titarchuk 1980 and more recent generalized *compTT* model (Titarchuk 1994). In those cases the parameter of reflected component E_{cut}, the cutoff energy, has been frozen at the value $3kT_e$, where kT_e is a temperature of hot electrons as inferred from the model of the Comptonization. The value of optical depth parameter depends on the geometry assumed - in case of *compTT* we cite τ parameter for both spherical and disk geometries. It is well known that the cut-off at energies higher than $\sim 3kT_e$ is more abrupt in the spectrum of the Comptonized emission than the simple exponential cut-off, but we were not able to statistically significant state the difference because of source weakness. A Gaussian component with central energy 6.4 keV and FWHM 0.1 keV (frozen at these values) have been added to account for a iron line emission.

During an observation (#10) taken at Nov 17, 1998 very low flux from the source was detected by PCA experiment. The spectrum was found to be softer, with power law photon

index ∼2 in comparison with ∼1.5 during the outburst of 1997. This observation might represent quiescent state of GS1354–644 or the transition to that state.

4.1. Spectral changes study

To study spectral changes in more detail we have examined spectral ratios for single observations spectra divided by the spectrum of the observation with the maximal flux. This method allows us to avoid the uncertainties in PCA response matrix and to search for finer differences between spectra. The drift of detector parameters, however, can contribute an additional systematic error, when you compare the spectra obtained during long period of time.

Our observed ratios could all be approximated by a single power law E^{β} in spite of the complexity of initial spectra. We have used the power law index β for quantitative comparisons of ratios obtained. The results of such analysis for separate observations are presented on Table 5 and in Fig.8.

As have been mentioned above, slow change in parameters of PCA detectors with time could introduce errors into the analysis based on this technique. To estimate the level of systematic error, we applied the same technique to several Crab spectra taken during the period of GS1354–644 outburst. The results presented in Fig.8 demonstrate that the changes in Crab spectra, which can be attributed to the drift of detector's parameters, are much smaller than the effect found for GS1354–644. Spectra for single observations became relatively softer with time until the unexpected jump of hardness for the latest outburst observation. No clear correlation with flux level have been found, in fact, spectra for the same flux level, but obtained during different stage of the source evolution (for phase of rise and for phase of decline) have significantly different slopes of the ratio.

The same method has been applied for study of spectrum-flux dependence within single observation sessions. Here we should not worry about systematic errors discussed above, however, the method of data selection is important and may affect the results. The data have been filtered according to the total count rate from the source obtained in 16-sec intervals. Then for each observation two spectra have been built, integrated over high-flux and low-flux periods. Thanks to large chaotic variations of the flux we were able to collect sufficient amount of data for average flux levels, which were different by a factor of 1.5–2. Finally, the spectrum corresponding to higher fluxes has been divided by the spectrum corresponding to lower fluxes. As mentioned above, this method of data selection in principle can introduce some systematic errors, because most counts fall in the soft

part of the spectrum, and so one could expect to get softer spectra correlated with higher flux levels. To check the importance of this effect, we changed our selection criteria and re-filtered the data according to the flux levels detected above 10 keV. The results remain the same as before indicating that the effect we have detected is much stronger than the systematic contribution introduced by the selection criteria.

The obtained source spectral ratio is presented in the Fig .9. For comparison we present in the same Figure the spectral ratio for Cyg X-1 obtained by the same technique. The effect is qualitatively the same for Cyg X-1 as for GS1354–644. Power-law index of the ratio for Cyg X-1 was equal to $(-3.9 \pm 0.4) \times 10^{-2}$ for the observation of June 26, 1997, which we have analyzed. Power law fits for ratio spectra derived from this analysis are presented on Table 5. Power-law indexes for ratios of different observations are labeled β_1. The same parameter for ratios of spectra corresponding to high and low fluxes within single observation are presented under β_2 column title. While average spectra for single sessions do not show any correlation with measured flux, maximal-to-minimal ratios built for fast variability within one observation always have a slope $\beta_2 < 0$.

Systematic differences in the spectra obtained for higher and lower flux levels can be interpreted in various ways. The softening of overall spectrum may be due to the increase in the relative contribution of shots, with softer intrinsic spectrum than the underlying constant. The underlying continuum, in turn, may be formed by the sum of shorter shots, with harder spectra (this possibility is discussed, e.g. by Revnivtsev, Gilfanov & Churazov 1999). Another model is that low energy shot emission changes the temperature of hot plasma cloud responsible for the Comptonization and generation of hard emission. Besides, it can be suggested that shot spectra evolve with time and the higher flux parts of the shots have softer spectra. One may think about other plausible explanations of the observed phenomena.

We believe that spectral ratios are quite sensitive to subtle changes in parameters of the system. Application of this method to the long-term trend of the source spectrum shows the softening of the spectrum with time (except of the observation #9). It means that in our case the spectrum of the system is not directly correlated with the overall flux level (or luminosity value). Hardness-flux anti-correlation has been detected for short-term flux variations within one session, but has not been detected when comparing the spectra for different observations. We would like to mention that the latest observation of 1997 outburst, which breaks the overall pattern, likely corresponds to the secondary maximum or 'kick' in the light curve. The observation #10 performed in a year after the maximum of 1997 outburst showed significantly softer spectrum with flux more than two order of magnitude below the peak value.

5. Discussion

5.1. State of the system

High and low spectral states first identified in Cyg X-1 (Tananbaum et al. 1972) have been since observed in a number of X-ray binaries. Typical spectrum of a black hole binary in *high* state is formed by a soft thermal component and a hard power-law tail. The spectrum of *low* state is approximately a single power-law component with an exponential cut-off at higher energies. More detailed description of typical spectral states of X-ray binaries can be found elsewhere (e.g. Tanaka & Shibazaki 1996).

Studies of aperiodic time variability in black hole candidates provided another dimension to this phenomenological pattern. In particular, a third, very-high, state has been recognized (Miyamoto et al. 1991, 1994; Ebisawa et al. 1994). The temporal variability in this state is characterized by the presence of a 3-10 Hz QPO peak, plus either a band-limited noise or a weaker power law noise component (Belloni et al. 1997).

The hard power law like energy spectrum with a slope $\sim$1.5, as detected from GS 1354–644 during its 1997 outburst, is a clear indication that the source was in a hard/low spectral state. The character of rapid variability, absence of QPO, and power spectrum shape provides an additional prove for this statement. The type of fast X-ray variability and power spectra of GS 1354–64 looks qualitatively the same as was observed from other black hole candidates in low/hard state (e.g. Nowak et al. 1999a; Nowak, Wilms & Dove 1999; Grove et al. 1998). Such type of X-ray variations has been recognized as "canonical" for these systems in low state (Miyamoto et al. 1992). Furthermore, neutron star binaries in low state appeared to demonstrate fast variability very similar to black holes (e.g. Olive et al. 1998a; Ford et al. 1999). However, when black hole systems are in other - high or very high - states, their power spectra are distinctly different (van der Klis 1995; Belloni et al. 1997).

GS1354–644 was detected with Ginga in 1987 in its high/soft state (Kitamoto et al. 1990). We report here that in 1997-1998 the same source was in low/hard state. This confirms the earlier identification of the source as black hole candidate and also confirms that both high/soft and low/hard states are generic for this group of X-ray sources. In fact, all properties of GS1354–644, which we revealed in our analysis are very similar with properties of other sources of similar nature, both persistent and transient.

5.2. Geometry of the system

The energy spectrum of the source supports the model of low energy photons being Comptonized in a hot plasma cloud. An accretion disk reveals itself in the form of the fluorescent iron line emission detected at ∼6.4 keV and the reflected continuum detected at 15-20 keV. Equivalent width of the line and relative significance of the reflected component are both consistent with the assumptions that they are formed by a reflection of harder X-ray emission from the cold plasma, which according to the commonly accepted picture, forms an optically thick accretion disk around the compact object. It is rather straightforward to assume that the emitting region is composed of such a disk with a hot optically thick corona, responsible for the Comptonization of soft photons up to tens of keV. An exact geometrical configuration of the system remains unclear and is an interesting subject to explore.

The combination of cold accretion disk with hot corona is the most popular model for an interpretation of observations of Galactic black holes in their low/hard spectral state. A slab geometry for such a system, where the accretion disk is sandwiched between two flat corona layers, which had been widely discussed several years ago (Haardt & Maraschi 1991, Haardt 1993), has not been able to fit the spectra observed in self-consistent manner (see eg. Dove, Wilms & Begelman 1997). Other models typically suggest a spherical hot corona (Kazanas, Hua & Titarchuk 1997) or advection-dominated accretion flow (Narayan 1996) at radii smaller than the inner radius of the thick accretion disk. Seed soft photons could be generated in the accretion disk (Dove, Wilms & Begelman 1997, Dove et al. 1998) or inside the hot cloud (suggested by Narayan 1996 to be synchrotron/cyclotron photons). The former models suggest an external illumination of the up-scattering region, while the latter assume an internal source embedded into the hot plasma itself.

The optical depth parameter $\tau \sim 4 - 5$ inferred from our spectral fits (*compST* and *compTT* models in spherical geometry) is model and geometry and model dependent and can not be considered as a direct measurement of the optical depth. However, the obtained value of τ still indicates that the source of the seed photons is most possibly located inside the hot cloud. In case of external illumination of the Comptonization region by soft photons originated from the accretion disk, the optical depth parameter would be expected of ∼1 even for high intrinsic values of τ in hot cloud itself. Partial overlap of the disk by the corona region may solve the puzzle, but the physical basis for such a configuration has still to be explored.

Additionally, if the characteristic frequency of the Compton cloud is of the order of Hz, then the cloud should be of huge size, and this in turn causes severe problems with an energy balance (see e.g. Nowak et al. 1999a). It looks more likely that the breaks in

PDS could be associated with the intrinsic duration of the seed shots. They also could be related with some geometrical parameters of the system, such as the radius of the accretion disk, and with typical times, as the Keplerian period of the disk rotation at this radius. In PDS of GS1354–644 the first break frequency is in anti-correlation with flux. This might reflect changes in some of the system parameters. For example, the inner radius of the disk might move closer to the compact object when the mass accretion rate is growing and the luminosity of the source is increasing, and move outward during the decrease of mass accretion rate, corresponding to the decline in the emitted flux. The magnetic field in the interior of the accretion flow is amplified by the disk differential rotation, and therefore, the characteristic time of the magnetic shots can also be connected with the period of rotation. If shots originate from geometrically small areas at different radii in the accretion disk, then the Keplerian rotation of the disk would modulate the shot signal with the frequencies of modulation corresponding to the range of typical radii.

5.3. Dependence of fractional variability on energy

Energy dependence of the integrated fractional variability of GS1354–644 on energy presented in Fig.4 clearly indicates the decrease of *rms* variability with energy, which can be approximated by a power law $rms \sim E^{-0.07}$.

It is worth mentioning that similar dependences have been found for Nova Per 1992 (Vikhlinin et al. 1995), Cyg X-1(Nowak et al. 1999a), and GX339–4(Nowak, Wilms & Dove 1999) - all Galactic black hole binaries - when observed in low/hard state. In contrast, *the increase of the fractional variability with energy* has been detected for some X-ray bursters – e.g. 1E1724-3045 (Olive et al. 1998a), 4U1608-522 (Yu et al. 1997) in their low/hard state. This apparent difference in the properties of Galactic black hole and neutron star systems is remarkable, because these systems, when in low/hard state, resemble each other in many other observational features. This fact motivated us to perform our own study based on publicly available RXTE data. X-ray bursters 4U1705-44, SLX 1735-269, SAX J1808-3659, 4U1728-34 (GX 354-0) and 4U0614+091, together with the aforementioned systems 1E1724-3045 and 4U1608-522, have been included in a handful of sources under analysis.

Approximations of *rms* vs. energy dependence by power-law fit for some Galactic X-ray binaries is presented on Table 6. All observations selected were performed, when objects were in their low/hard state. In cases of GX339-4 and Terzan 2 data were taken from Nowak, Wilms & Dove 1999 and Olive et al. 1998a respectively. We did not present here data for GRO J0422+32(Nova Per 1992; Vikhlinin et al. 1995), because even though

they demonstrate the same overall trend (decrease of rms vs. energy for BH systems), the energy band was in this case very different from other observations. We would like to stress that simple power law provided in some cases quite poor fit for the data, but we used it anyway to understand the tendency (is *rms* decreased, increased or stayed constant with energy increase). The results show clearly that the sign of best fit power-law approximation is negative for all black hole binaries and positive for systems with neutron stars. The most evident correlation of fractional variability with energy is detectable at least for energies below ∼15 keV. In fact, it seems that the fractional variability has a broad maximum at energies 10-20 keV for many X-ray bursters, whereas for black holes the maximal *rms* values correspond to the lower energy limit for the given energy band (∼ 3–20 keV). This might be an indication that the formation of similar spectra in black hole and neutron star systems has in fact some fundamental differences.

Whatever is the actual physical reason, the difference observed is quite interesting, because of the large similarity in the properties of black hole and neutron star systems in low/hard state, reported in recent publications (e.g. Berger & van der Klis 1998; Revnivtsev et al. 1998; Olive et al. 1998a). If confirmed, this dependence may become an important new tool for determining the type of compact object in Galactic binaries from X-ray observations.

6. Conclusions

An analysis of observations of recurrent X-ray transient GS1354-644 by RXTE satellite provided us with several interesting results.

The observations were made during a minor outburst of the system. The overall light curve is triangular, and PCA/HEXTE observations have been carried out both during the rise of the flux and in the decay phase. Dramatic fast variability has been studied in terms of a shot noise model, which is commonly used for interpretation of this type of variability. The PDS spectrum can be approximated by the sum of 2-3 components, each corresponding to a specific type of shot. Two the most prominent ones are peaked around 0.02–0.09 Hz and 2.3–2.9 Hz correspondingly. For several first observations the addition of the third, intermediate component are statistically justified. The flux density distribution analysis showed that the longest shots rate is about 0.3 shots per second, they contribute 30–50% to the total flux from the source, and each of them gives as much as 200–500 counts as detected by PCA. Short shots are more frequent (∼ 10–15 shots/s) and proportionally weaker, their sum contribution to the total flux is similar to the contribution of longer shots. The rest of the flux if any can be attributed to the constant emission and to the

shots of intermediate duration.

In general, the rapid time variability of the source X-ray flux is very similar to what was observed in low/hard state for other Galactic black hole systems, as Cyg X-1, Nova Persei 1992, GX 339-4 etc.

The spectrum of the source obtained by PCA and HEXTE in an series of observations is also clearly the hard/low state spectrum as observed in many Galactic black hole binaries. The overall power-law-with- high-energy-cutoff shape can be approximated by Comptonization models based on up-scattering of soft photons on energetic electrons in a hot plasma cloud. In order to fit the data, an additional component describing the spectrum reflected from cold material with rather strong line of iron fluorescent emission must be included into the model. Both the equivalent width of the line and the intensity of the reflected component are consistent with the assumption of the reflection of hard X-ray emission from a cold, optically thick accretion disk.

To examine finer changes in the detected spectrum, we analyzed ratios of the spectra obtained. This technique demonstrated an overall softening of the spectrum during the outburst, except for the last observation, which was obtained during the secondary maximum on the light curve. At shorter time scales we also detect a softening of the spectrum at higher flux level, when we compare spectra corresponding to high and low flux levels within a given observation.

According to earlier studies and the results of this work, an anti-correlation of fractional variability with energy is typical for Galactic black holes in their low spectral state (e.g. Nowak et al. 1999a, Vikhlinin et al. 1995), but a positive correlation is typical for neutron star systems (also in low state; e.g. Olive et al. 1998a). Our analysis, performed with RXTE archival data for several sources, confirmed this difference in the energy dependence of rms variability for black hole and neutron star binaries. Taking into account the reported similarity in spectra and rapid variability for both types of systems in their low/hard state, this difference can be very useful for segregating neutron star binaries from black hole systems.

The research has made use of data obtained through the High Energy Astrophysics Science Archive Research Center Online Service, provided by the NASA/Goddard Space Flight Center.

MR is thankful to Dr.M.Gilfanov for extremely helpful discussions. KB is glad to acknowledge valuable comments by Prof.L.Titarchuk and Dr.S.Brumby. It is a must to regard anonymous ApJ referee for his/her careful reading of the manuscript and numerous important remarks, which helped us to improve significantly the quality of the paper.

REFERENCES

Basko, M., Sunyaev, R., Titarchuk, L. 1974, A&A, 31, 249

Barret, D., Grindlay, J.E., Harrus, I.M., & Olive, J.F. 1998, A&A, submitted, (astro-ph/9810463)

Belloni, T., & Hasinger, G. 1990, A&A, 230, 103

Belloni, T., van der Klis, M., Lewin, W.H.G., van Paradijs, J., Dotani, T., Mitsuda, K., & Miyamoto, S. 1997, 322, 857

Berger, M., & van der Klis, M. 1998, A&A, 340, 143

Bradt, H.V., Rothschild, R.E., & Swank, J.H. 1993, A&AS, 97, 355

Buxton, M., Vennes, S., Ferrario, L., & Wickramasinghe, D.T. 1998, IAU Circ.6815

Castro-Tirado, A.J., Ilovaisky, S., Pedersen, H., Gonzalez, J.-F., Pizarro, M., Miranda, J., & Boehnhardt, H. 1997 IAU Circ.6775

Chen, Wan, Shrader, C.R., & Livio, M. 1997, ApJ, 491, 312

Dove, J.B., Wilms, J., & Begelman, M.C. 1998, ApJ, 487, 747

Dove, J.B., Wilms, J., Nowak, M.A., Vaughan, B.A., & Begelman, M.C. 1998, MNRAS, 298, 729

Ebisawa, K., Ogawa, M., Aoki, T., Dotani, T., Takizawa, M., Tanaka, Y., Yoshida, K., Miyamoto, S., Iga, S., Hayashida, K., Kitamoto, S., & Terada, K. 1994, PASJ, 46, 375

Fender, R. P., Tingay, S. J., Higdon, J., Wark, R., & Wieringa, M. 1997, IAU Circ.6779

Ford, E.C., van der Klis, M., Mendez, M., van Paradijs, J., & Kaaret, P. 1999, ApJL, 512, L31

Francey, R.J. 1971, Nature Phys.Sci., 229, 228

George, I.M., & Fabian, A.C. 1991, MNRAS, 249, 352

Grove. J. E., Strickman, M. S., Matz. S. M., Hua, X.-M., Kazanas, D., Titarchuk, L., 1999, ApJ, 502, 45L

Guainazzi, M., Parmar, A.N., Segreto, A., Stella, L., dal Fiume, D., & Oosterbroek, T. 1998, A&A, 339, 802

Jahoda K. 1998a, http://lheawww.gsfc.nasa.gov/ users/ keith/ pcarmf.html

Jahoda K. 1998b, http://lheawww.gsfc.nasa.gov/users /keith/pcarmf_ft41.erratum

Haardt, F. 1993, ApJ, 413, 680

Haardt, F., & Maraschi, L. 1991, ApJ, 380, L51

Harmon, B.A., Zhang, S.N., Wilson, C.A., et al. 1994, in: The 2nd Compton Symp., ed. C.E.Fichtel, N.Gehrels, & J.P.Norris (New York: AIP), 210

Harmon, B.A., & Robinson, C.R. 1998, IAU Circ.6774

Harries, J.R., McCracken, K.G., Francey, R.J., & Fenton, A.G. 1967, Nature, 215, 38

Heindl, W., Blanco, P., Gruber, D., Pelling, M., Macdonald, D., Marsden, D., & Rothschild, R. 1997, IAU Circ.6790

Kazanas, D., Hua, X.-M., & Titarchuk, L. 1997, ApJ, 480, 280

Kitamoto, S., Tsunemi, H., Pedersen, H., Ilovaisky, S.A., & van der Klis, M. 1990, ApJ, 361, 590

Lochner, J., Swank J., & Szymkowiak A. 1991, ApJ, 376, 295

Lochner, J., & Roussel-Dupre, D. 1994, ApJ, 435, 840

Magdziarz, P., & Zdziarski, A.A. 1995, MNRAS, 273, 837

Makino, F. 1987, IAU Circ. 4342

Markert, T.H., Canizares, C.R., Clark, G.W., Hearn, D. R., Li, F. K., Sprott, G. F., & Winkler, P. F. 1977, ApJ, 218, 801

Mitsuda, K., Inoue, H., Koyama, K., Makishima, K., Matsuoka, M., Ogawara, Y., Suzuki, K., Tanaka, Y., Shibazaki, N., & Hirano, T. 1984, PASJ, 36, 741

Miyamoto, S., Kimura, K., Kitamoto, S., Dotani, T., & Ebisawa, K. 1991, ApJ, 383, 784

Miyamoto, S., Kitamoto, S., Iga, S., Negoro, H., & Terada, K. 1992, ApJ, L21, 391

Miyamoto, S., Kitamoto, S., Iga, S., Hayashida, K., & Terada, K. 1994, ApJ, 435, 398

Narayan, R. 1996, ApJ, 462, 136

Nowak, M.A., Vaughan, B.A., Wilms, J., Dove, J.B., & Begelman, M.C. 1999a, ApJ, 510, 874

Nowak, M., Wilms, J., Vaughan, B.A., Dove, J.B., & Begelman, M.C. 1999b, ApJ, preprint (astro-ph/9810406)

Nowak, M., Wilms, J. & Dove, J. 1999, ApJ, preprint (astro-ph/9812180)

Olive, J.F., Barret, D., Boirin, L., Grindlay, J.E., Swank, J.H., & Smale, A.P. 1998, A&A, 333, 942

Olive, J.F., Barret, D., Boirin, L., et al. 1998, Submitted for publication in Advances in Space Research, Proc. of the 32nd COSPAR Meeting held in Nagoya, 12-15 July, 1998, "Broad band Spectra of Cosmic X-ray sources"

Pedersen, H., Ilovaisky, S., & van der Klis, M. 1987, IAU Circ. 4357

Pottschmidt, K., Wilms, J., Nowak, M.A., et al. 1998, to be published in "Highlights of X-Ray Astronomy, a symposium in honour of Joachim Truemper" (B. Aschenbach et al., eds.), MPE Report

Rothschild, R.E., Blanco, P.R., Gruber, D.E., Heindl, W.A., Macdonald, D.R., Marsden, D.C., Pelling, M.R., Wayne, L.R., & Hink, P.L. 1998, ApJ, 496, 538

Remillard, R., Marshall, F. & Takeshima, T. 1998, IAU Circ.6772

Revnivtsev, M., Gilfanov, M., Churazov, E., & Sunyaev, R. 1998, To appear in Proc. of 3^{rd} INTEGRAL Workshop (astro-ph/9812186)

Revnivtsev, M., Gilfanov, M., & Churazov, E. 1999, A&AL, submitted

Seward, F.D., Page, C.G., Turner, M.J.L., & Pounds, K. 1976, MNRAS, 177, 13

Shakura, N.I., & Sunyaev, R.A. 1973, A&A, 24, 337

Shakura, N., & Sunyaev, R. 1988, AdSpR, 8, 135

Shapiro, S.L., Lightman, A.P., & Eardley, D.M. 1976, ApJ, 204, 187S

Soria, R., Bessell, M.S.& Wood, P., IAU Circ.6781

Stark 1998, http://lheawww.gsfc.nasa.gov/ ∼stark/ pca/ pcabackest.html

Sunyaev, R., & Shakura, N. 1986, SvAL, 12, 117

Sunyaev, R.A., & Titarchuk, L.G. 1980, A&A, 86, 121 (ST80)

Sunyaev, R.A., Borozdin, K.N., Aleksandrovich, N.L., Arefiev, V.A., Kaniovsky, A.S., Efremov, V.V., Maisack, M., Reppin, C., & Skinner, J.K. 1994, Astron.Lett., 20, 890

Sutherland, P.G., Weisskopf, M.C., & Kahn, S.M. 1978, ApJ, 219, 1029

Tanaka, Y., & Lewin, W.H.G. 1995, in *X-ray Binaries* eds. W.H.G.Lewin, J.van Paradijs, & E.P.J. van den Heuvel, Cambridge Univ.Press, 126

Tanaka, Y., & Shibazaki, N. 1996, Ann.Rev.Astron.Astroph., 34, 607

Tananbaum, H., Gursky, H., Kellogg, E., Giacconi, R., & Jones, C. 1972, ApJ, 177, L5

Terrell, N.J. 1972, ApJ, 174, L35

Titarchuk, L.G. 1994, ApJ, 434, 570

van der Klis, M. 1995, in *X-ray Binaries* eds. W.H.G.Lewin, J.van Paradijs, & E.P.J. van den Heuvel, Cambridge Univ.Press, 252

van der Klis, M. 1989, in *Timing Neutron Stars*, H.Oegelman and E.P.J. van den Heuvel(eds.), Kluwer, Dordrecht (NATO ASI Series C 262), 27

Vikhlinin, A., Churazov, E., Gilfanov, M., Sunyaev, R., Finoguenov, A., Dyachkov, A., Kremnev, R., Sukhanov, K., Ballet, J., Goldwurm, A., Cordier, B., Claret, A., Denis, M., Olive, J.F., Roques, J.P., & Mandrou, P. 1995, ApJ, 441, 779

Wijnands, R., & van der Klis, M. 1998, preprint (astro-ph/9810342)

Wilms, J., Nowak, M., Dove, J., Fender, R., Matteo, T. 1999, accepted in ApJ (see also astro-ph/9904123)

White, N., Stella, L., & Parmar, A. 1988, ApJ, 324, 363

Wood, K.S., Meekins, J.F., Yentis, D.J., Smathers, H.W., McNutt, D.P., Bleach, R.D., Friedman, H., Byram, E.T., Chubb, T.A., & Meidav, M. 1984, ApJ Suppl., 56, 507

Yu, W., Zhang, S.N., Harmon, B.A., Paciesas, W.S., Robinson, C.R., Grindlay, J.E., Bloser, P., Barret, D., Ford, E.C., Tavani, M., & Kaaret, P. 1997, ApJ, 490, L153

Zhang, W., & Jahoda, K. 1996, http://lheawww.gsfc.nasa.gov/ users/ keith/ deadtime/deadtime.html

Table 1: RXTE observations of GS 1354-644.

#	Obs. ID	Date	Start time	TJD[t]	Exposure, sec.	
					PCA	HEXTE[a]
1	20431-01-01-01	18/11/97	00:28:32	10770.019	1672	-
2	20431-01-02-01,3	19/11/97	13:11:28	10771.553	5920	1812
3	20431-01-03-00	22/11/97	09:39:28	10774.402	6592	2601
4	20431-01-04-00	05/12/97	05:00:48	10787.209	6809	2053
5	20431-01-05-00	12/12/97	19:21:20	10794.806	6119	1969
6	30401-01-01-00	27/12/97	14:39:28	10809.610	6516	1896
7	30401-01-02-00	04/01/98	17:47:12	10817.741	7349	2321
8	30401-01-03-00	12/01/98	15:04:32	10825.628	6355	1932
9	30401-01-04-00	26/01/98	12:07:28	10839.505	6594	2191
10	30401-01-05-00	17/11/98	10:00:14	11134.583	4109	1597[r]

[a] - Dead time corrected exposure for each cluster of HEXTE detectors.

[r] - This observation was in real-time format, so we could not correct it for the dead time

[t] - TJD=JD-2440000.5, where JD is Julian Date or number of days since Greenwich mean noon on Jan 1, 4713 B.C.

Table 2: Best-fit parameters for power spectra approximation (3–60 keV, 10^{-3}–20 Hz),

Obs.	rms^a_{total} %	$Break_1$ 10^{-2} Hz	rms^a_1 %	$Break_2$ Hz	rms^a_2 %	$Break_3$ Hz	rms^a_3 %	$\chi^2_{100dof}/100$
1	39.2 ± 2.6	8.2 ± 0.9	27 ± 2	0.39 ± 0.23	16 ± 6	2.31 ± 0.18	23 ± 1	1.4
2	32.5 ± 1.1	2.5 ± 0.2	16 ± 1	0.36 ± 0.05	15 ± 1	2.27 ± 0.10	20 ± 1	1.6
3	31.8 ± 1.3	2.6 ± 0.2	14 ± 1	0.47 ± 0.06	16 ± 1	2.55 ± 0.10	23 ± 1	1.2
4	31.5 ± 1.2	5.8 ± 0.4	18 ± 1	0.72 ± 0.17	12 ± 1	2.87 ± 0.16	23 ± 1	1.1
5	29.8 ± 1.2	7.5 ± 0.3	19 ± 1	-	-	2.30 ± 0.04	23 ± 1	1.5
6	29.4 ± 1.7	9.5 ± 0.3	19 ± 1	-	-	2.37 ± 0.05	23 ± 1	1.4
7	28.9 ± 2.3	9.6 ± 0.3	18 ± 2	-	-	2.48 ± 0.05	23 ± 1	1.2
8	33.2 ± 2.6	10.1 ± 0.3	23 ± 2	-	-	2.50 ± 0.06	24 ± 2	1.3
9	34.9 ± 4.1	9.1 ± 0.3	27 ± 2	-	-	2.27 ± 0.07	22 ± 2	1.2
10	< 25							

- The power spectrum was approximated by a three component model. Each component is a function $\sim \frac{1}{1+(\frac{f}{break_x})^2}$, that corresponds to the simple exponential shot power spectrum. In the 6^{th}–9^{th} observations the middle component was not significant.

[a] - The systematic uncertainty of the background rate was included when calculating the errors of the rms values of all components.

Table 3: Spectral fit parameters for GS 1354–644.

Pexrav (power law with cutoff + reflection) + Gauss							
Obs.#	α	E_{cutoff}, keV	$\Omega/2\pi^a$		EW, eV	F^b	$\chi^2_{324dof}/324$
2–5	1.52 ± 0.05	123 ± 8	0.56 ± 0.04		58 ± 12	59.5 ± 0.5	0.74
6–9	1.54 ± 0.07	230 ± 20	0.41 ± 0.04		53 ± 12	36.5 ± 0.04	0.99
Broken power law with cutoff + Gauss							
Obs.#	α_1	E_{break}, keV	α_2	E_c, keV	EW, eV	F^b	$\chi^2_{323dof}/323$
2–5	1.41 ± 0.02	10.1 ± 0.3	1.12 ± 0.02	57 ± 3	54 ± 12	58.7 ± 0.5	0.75
6–9	1.46 ± 0.02	10.4 ± 0.3	1.18 ± 0.02	84 ± 5	57 ± 12	36.3 ± 0.04	0.92
CompTT^c + reflection + Gauss							
Obs.#	kT_e, keV	τ	$\Omega/2\pi^a$		EW, eV	F^b	$\chi^2_{324dof}/323$
2–5	28 ± 2	2.1 ± 0.1(disk) 4.8 ± 0.2(sphere)	0.29 ± 0.05		63 ± 15	57.5 ± 0.5	0.98
6–9	33 ± 2	1.9 ± 0.1(disk) 4.3 ± 0.2(sphere)	0.3 ± 0.07		57 ± 12	35.5 ± 0.5	1.1
CompST(sphere) + reflection + Gauss							
Obs.#	kT_e, keV	τ	$\Omega/2\pi^a$		EW, eV	F^b	$\chi^2_{324dof}/323$
2–5	23.6 ± 1.0	5.0 ± 0.1	0.55 ± 0.05		65 ± 12	54.3 ± 0.8	0.86
6–9	28.8 ± 1.0	4.5 ± 0.1	0.33 ± 0.05		50 ± 12	31.9 ± 0.8	0.92
Power law							
Obs.#	α	$F_{3-20keV}$	$F_{20-100keV}$				χ^2_{43dof}
10	2.0 ± 0.1	0.24 ± 0.04	< 1.2				0.64

- The width of the Gaussian line was frozen on the value 0.1 keV, comparable to the PCA energy resolution in this band; $cos(\theta)$ (θ - inclination angle) for the reflection component was frozen with the value 0.45

[a] - Error interval doesn't include potentially important effect of cross-calibration uncertainties between PCA and HEXTE experiments

[b] - The source flux in the energy band 3–170 keV in the units of 10^{-10} erg/s/cm^2. HEXTE normalization was adjusted to PCA one

[c] - For this model the optical depth was calculated for both sphere and disk geometries. CompST model assumed spherical geometry of Comptonizing plasma

Table 4: Parameters of HEXTE spectra approximation by power-law model (20–170 keV energy range).

	Power law with cutoff		
Obs.#	α	E_{cutoff}, keV	χ^2_{282dof}
2–5	1.13 ± 0.04	66 ± 4	234
6–9	1.05 ± 0.05	80 ± 8	292

- different clusters were fitted with different normalizations)

Table 5: Power-law fits of ratio spectra for GS1354–644 observations

#Obs.	Flux/Flux$_{ref}$,%	β_1^a,$\times 10^{-2}$	χ^2_{44}	Flux$_{max}$/Flux$_{min}$	β_2,$\times 10^{-2}$	χ^2_{44}
1	88 ± 1	3.6 ± 0.3	0.74	1.97 ± 0.01	-5.7 ± 0.8	0.85
2	88 ± 1	4.6 ± 0.3	1.01	2.35 ± 0.01	-5.7 ± 0.8	1.00
3	98 ± 1	2.7 ± 0.2	0.70	1.86 ± 0.01	-5.7 ± 0.4	1.13
4	-	-	-	1.83 ± 0.01	-6.8 ± 0.7	1.18
5	89 ± 1	-0.3 ± 0.2	0.73	1.95 ± 0.01	-6.2 ± 1.0	0.91
6	69 ± 1	-1.7 ± 0.3	0.72	1.59 ± 0.01	-3.6 ± 0.7	0.95
7	54 ± 1	-1.7 ± 0.2	1.01	1.57 ± 0.01	-2.9 ± 0.7	1.16
8	51 ± 1	-1.9 ± 0.2	0.75	1.41 ± 0.01	-2.3 ± 0.7	0.79
9	59 ± 1	8.4 ± 0.5	1.06	1.70 ± 0.01	-22 ± 2	1.02
10	2.2 ± 0.3	-59 ± 6	0.55	-	-	-

[a] – This value is of extreme accuracy as long as the response of the instrument is stable. Crab nebulae observations show that the slope of the spectrum on a time scale of 5 months remains the same with the accuracy $\sim 6 \times 10^{-3}$.

Table 6: Slopes of the dependence of fractional variability on energy (in ∼3–15 keV energy range) for some Galactic X-ray binaries observed in low/hard state.

Source	Type	Date	PL slope
GS 1354–644	BH	Nov 19, 1997	-0.07 ± 0.01
Cyg X-1	BH	Jun 26, 1997	-0.05 ± 0.005
GX 339-4	BH	Sep 19, 1997	-0.035 ± 0.01[a]
Terzan 2	NS	Nov 1996	$+0.25 \pm 0.04$[b]
GX 354-0	NS	Mar 3, 1996	$+0.08$[c]
SAX J1808.4-3658	NS	Apr 13, 1998	$+0.16 \pm 0.03$
4U1608-522	NS	Dec 27, 1996	$+0.6 \pm 0.3$
4U0614+091	NS	Jan 25, 1997	$+0.20 \pm 0.04$
4U1705-44	NS	Mar 29, 1997	$+0.13 \pm 0.05$
SLX 1735-269	NS	Feb-May, 1997	$+0.10 \pm 0.17$

[a] - taken from Nowak, Wilms & Dove 1999

[b] - taken from Olive et al. 1998a

[c] - the value is presented without the confidence interval because $rms - energy$ dependence in this case is clearly not simple power-law (see Fig.4a)

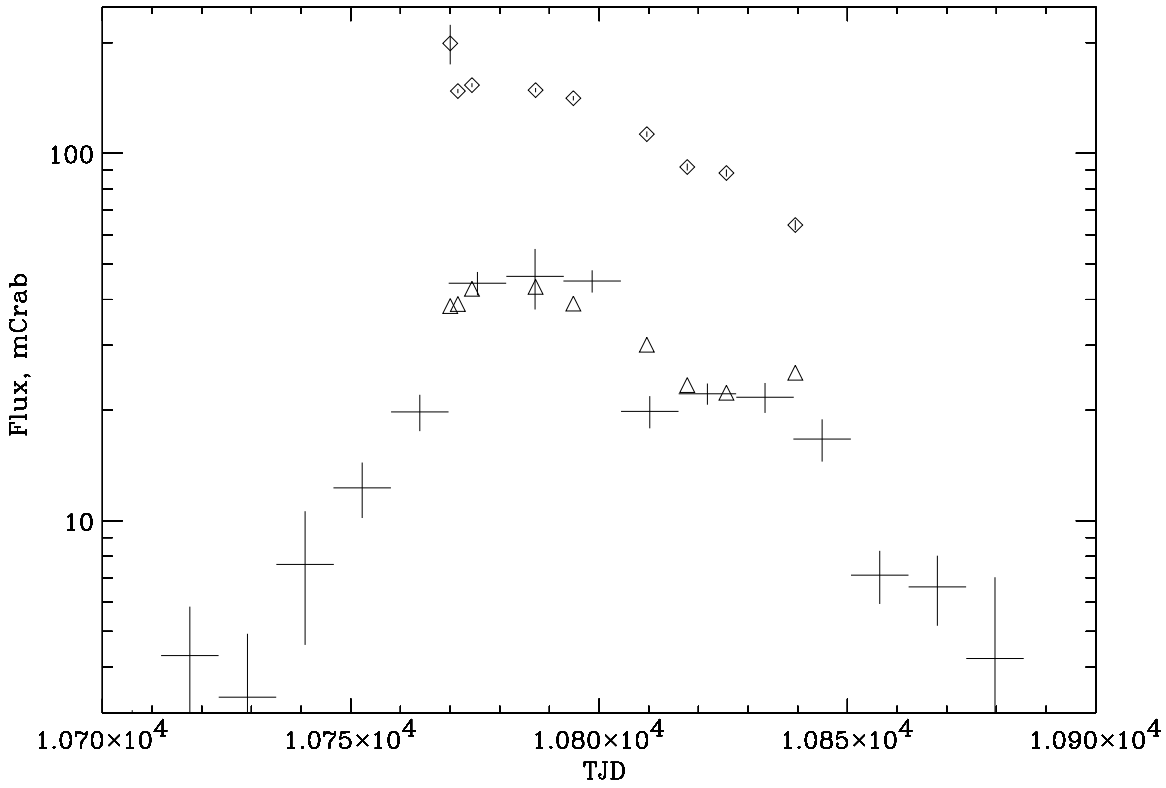

Fig. 1.— Light curve for the 1997-1998 outburst of GS 1354–644. Time axis in Truncated Julian Dates (TJD=JD-2440000.5). Crosses represent the ASM data (1.3–12.2 keV), open triangles - PCA data (3–20 keV), diamonds - HEXTE data (20–100 keV).

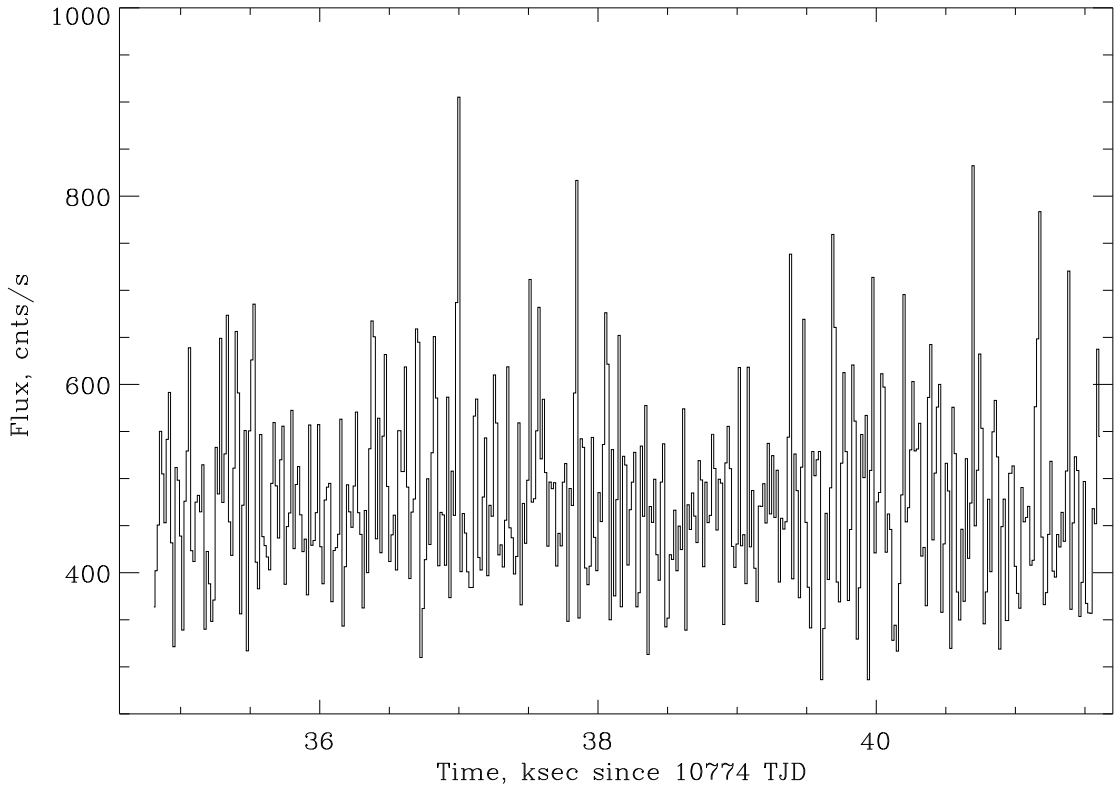

Fig. 2.— The characteristic light curve of GS 1354–644 during one observation as observed by PCA. Each bin corresponds to the flux collected in a 16-sec time interval. Statistical errors for each bin are negligible.

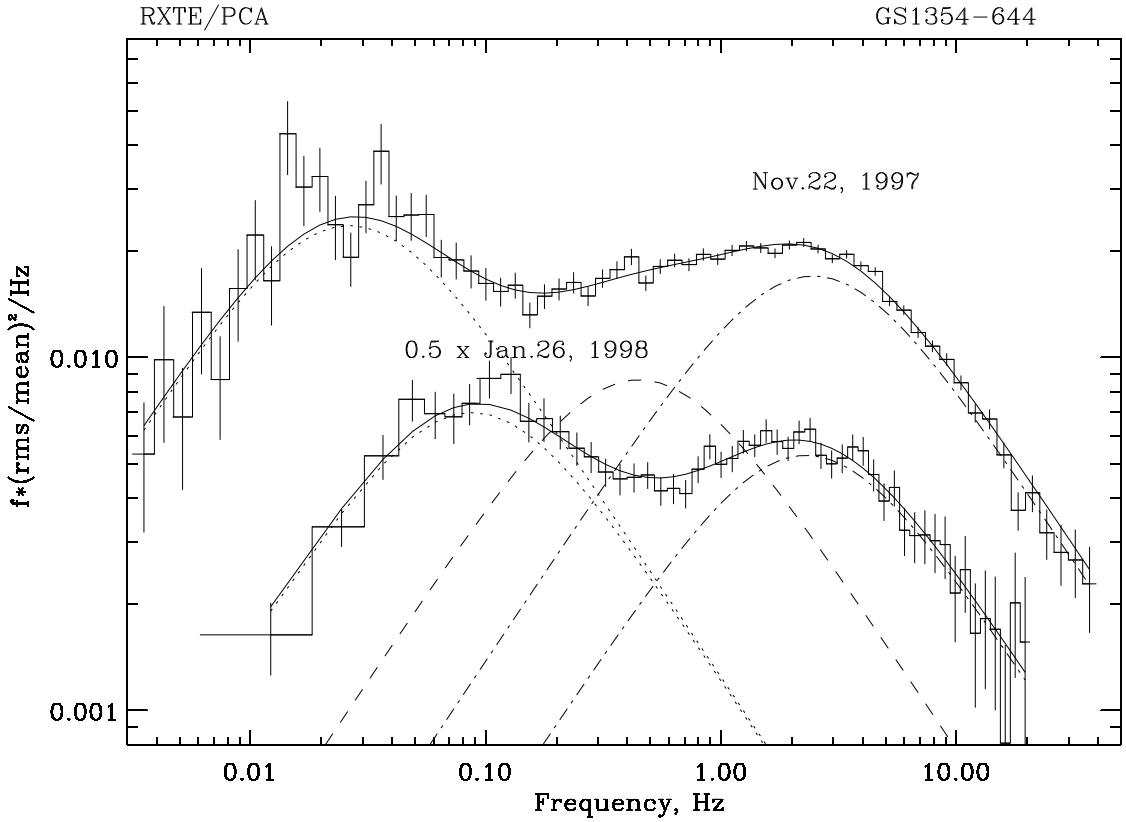

Fig. 3.— The power density spectra for two observations of GS1354–644 with PCA. Upper spectrum was obtained for the observation #3; lower one for #9. Three model components (see Table 3 and text) are shown by dotted, dashed and dash-dotted lines correspondingly for both observations. Data and model components for observation #9 (two-component model was applied in this case) were multiplied by 0.5 to avoid confusion with observation #3.

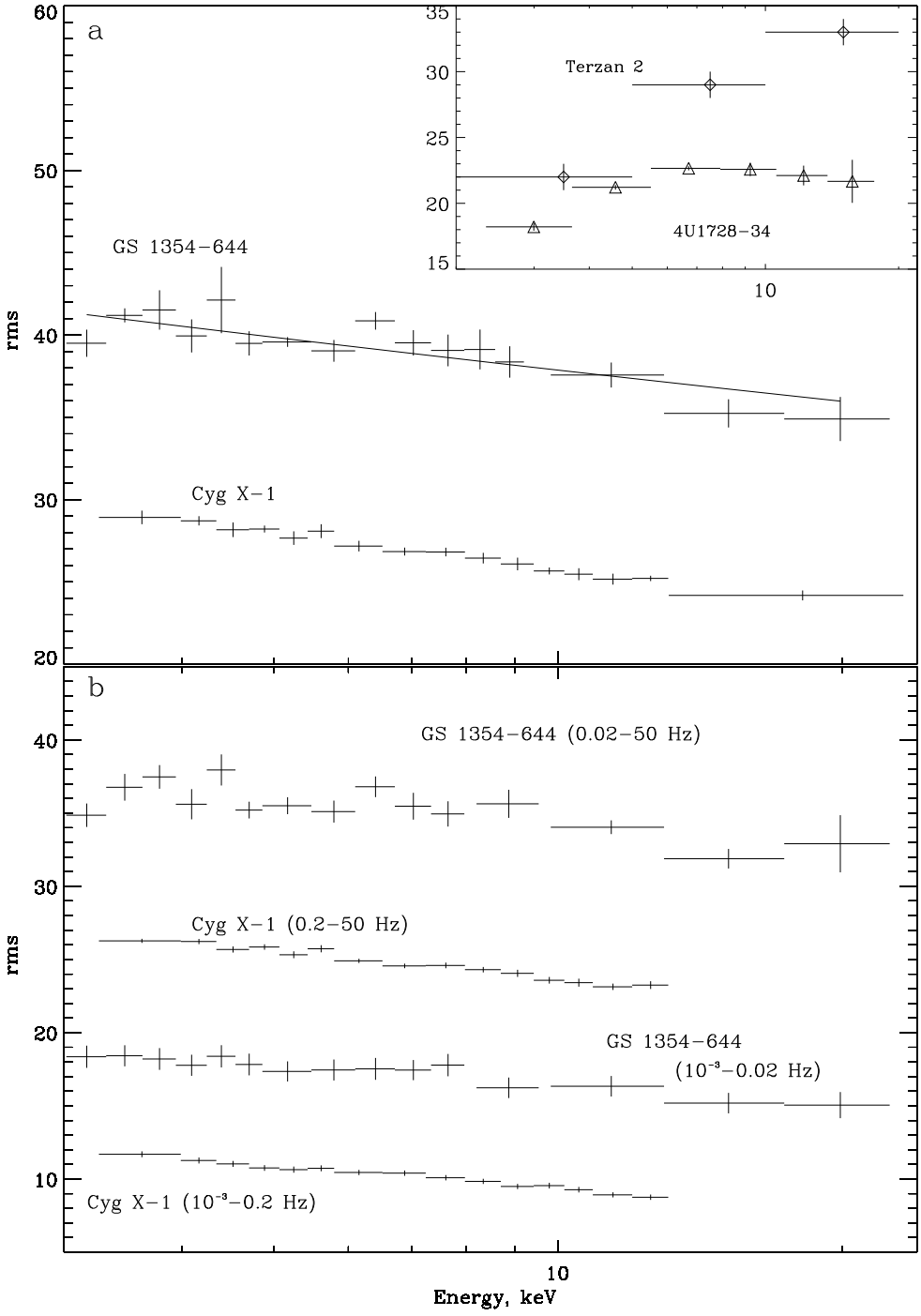

Fig. 4.— Upper panel(a): The dependence of the fractional variability of GS1354–644 flux integrated over the frequency range 10^{-3}–40 Hz on the energy of the photons (observation #3). Dependencies for Cyg X-1, 4U1728-34 and Terzan 2 (Olive et al., 1998a) are shown for the comparison. Lower panel(b): Energy dependence of the fractional variability values integrated over different frequency ranges (above and below the first break in PDS) for GS 1354–644 and Cyg X-1.

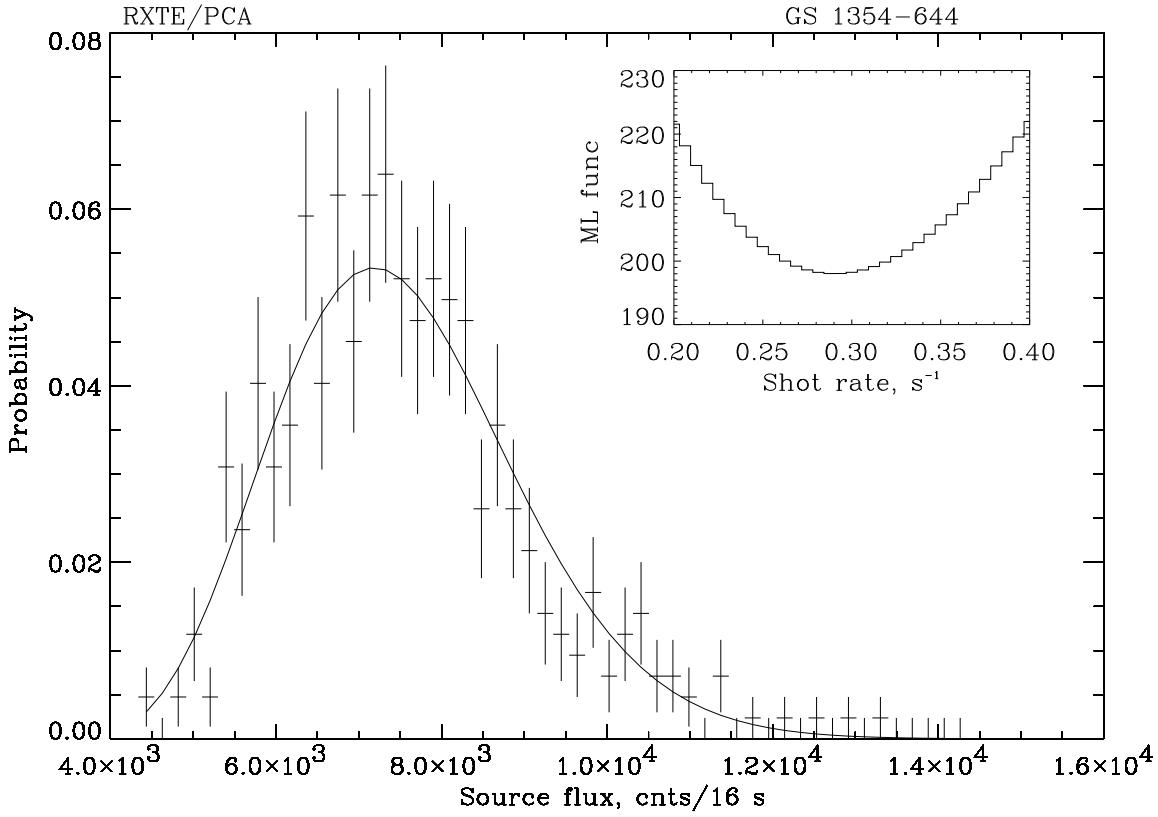

Fig. 5.— The distribution of the source flux, integrated over 16-sec intervals (observation #3). The dependence of the maximum likelihood function on shot rate is shown in the right upper corner. The best fit parameters are: the amplitude of single shot ~ 215 counts and shot rate ~ 0.3 shots/s.

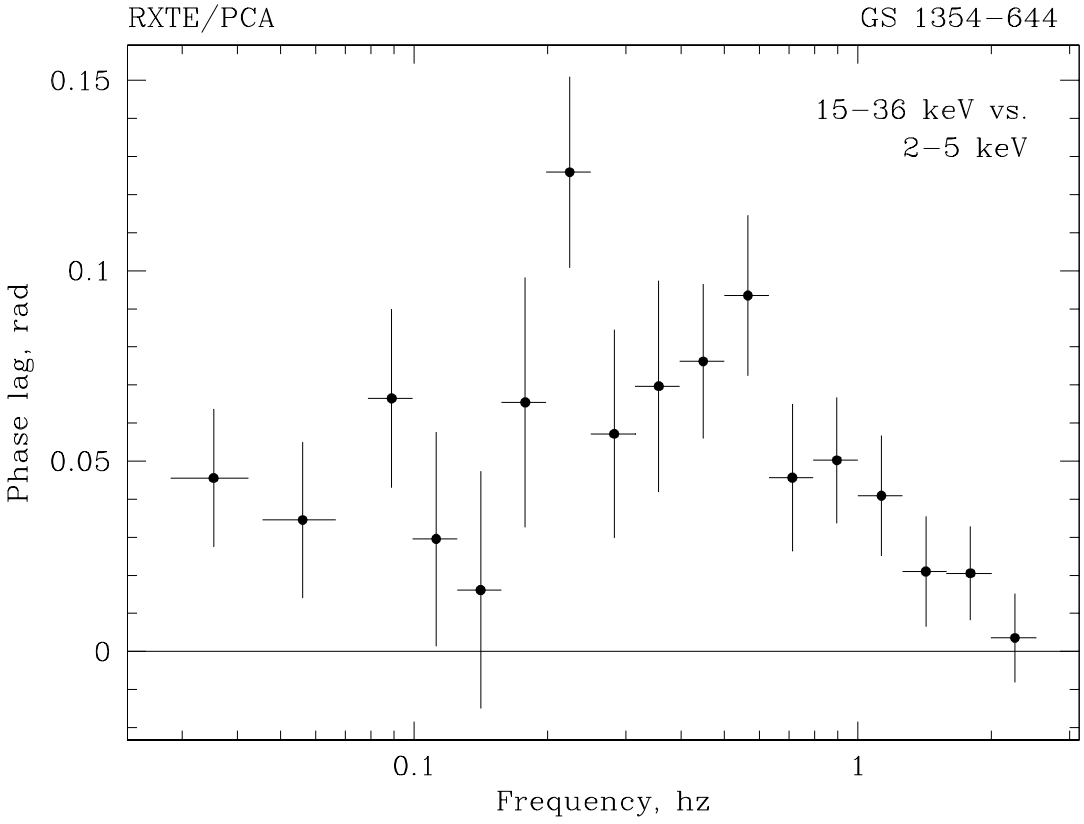

Fig. 6.— Phase lags, as a function of the Fourier frequency for 15–36 keV energy band vs. 2–5 keV energy band.

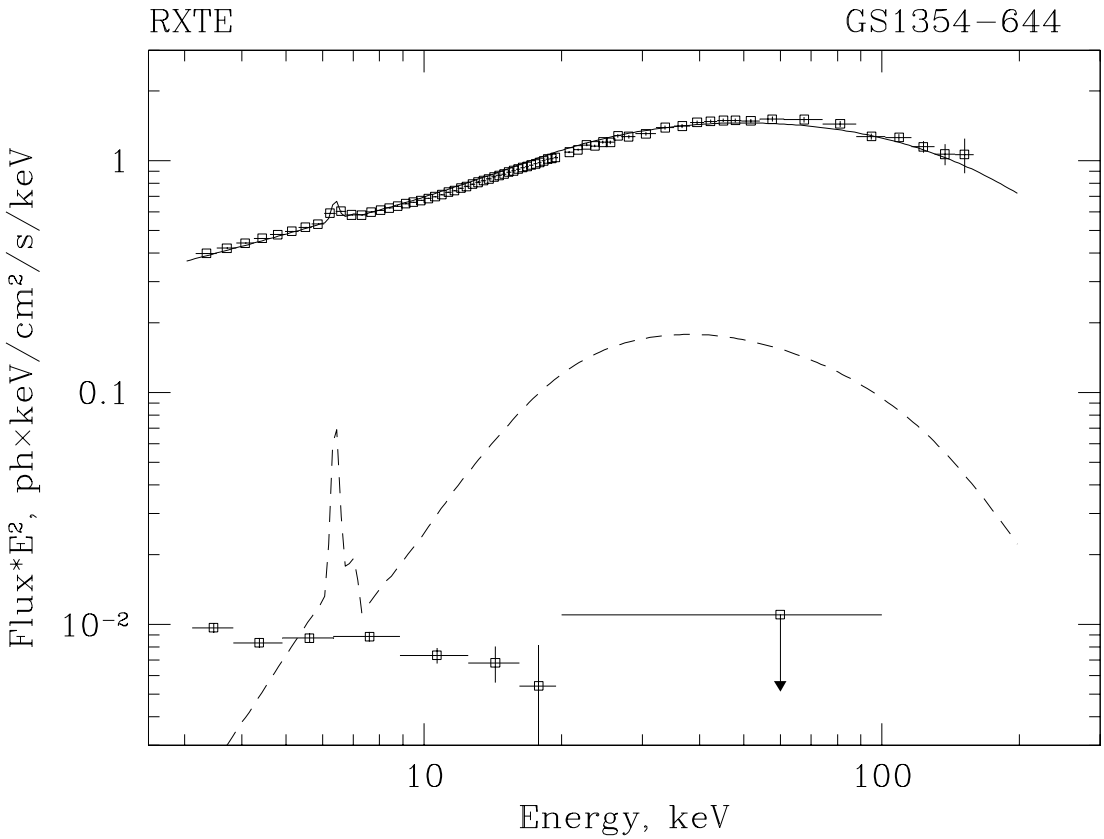

Fig. 7.— The energy spectra of GS 1354-644 during the maximum of the outburst and in quiescence. Upper spectrum is an average over the observations 3–5, lower one corresponds to the observation #10 - no detection in HEXTE energy band, 2σ upper limit is shown for energies above 20 keV. Solid line is a fit to the data by the model described in the text ($compST + reflection + Gauss$). Dashed line is the Compton reflected component and Fe K_α fluorescent line. Parameters of the fit are presented on Table 3.

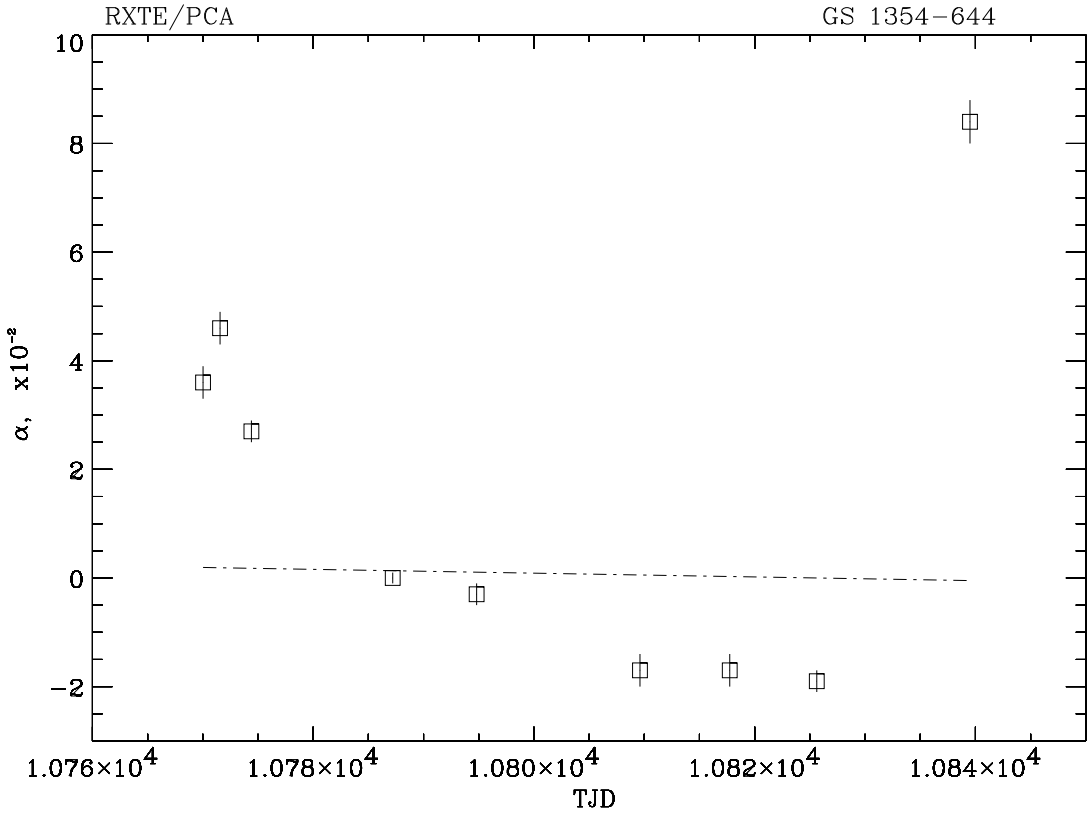

Fig. 8.— The dependence of the slope of the ratio spectra (see text) on time. The spectrum of observation #4 was used as a reference point. Dot-dashed line show the approximation to the trend for the Crab spectra analyzed.

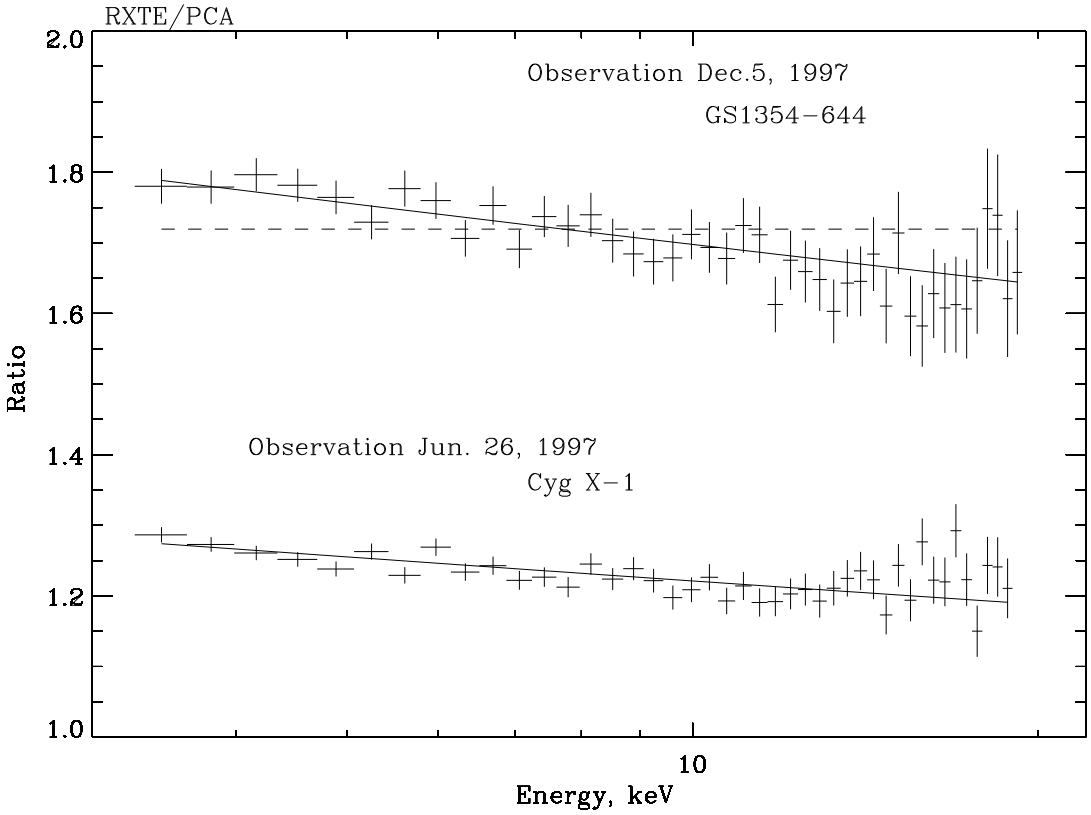

Fig. 9.— The 3-20 keV ratio of the spectra integrated over intervals with the higher and lower flux levels (observation #4). Similar ratio for Cyg X-1 is shown for comparison.